Supplemental Material to "Giant Kovacs-Like Memory Effect for Active Particles"

Rüdiger Kürsten, Vladimir Sushkov, and Thomas Ihle

(Dated: August 4, 2017)

NONLINEAR THEORY

In the following we give the derivation of Eq. (7). Consider a family of maps $F_\eta : \mathbb{R}^n \to \mathbb{R}^n$. In the present system the map F is given by Eq. (1). We assume that each map has a single globally attractive stable fixed point $\mathbf{x}^*_\eta$ such that $F_\eta(\mathbf{x}^*_\eta) = \mathbf{x}^*_\eta$. We define the shifted coordinate $\mathbf{y}$ and map G_η by

$$\mathbf{y} := \mathbf{x} - \mathbf{x}^*_{\eta_f}, \qquad G_\eta(\mathbf{y}) := F_\eta(\mathbf{y} + \mathbf{x}^*_{\eta_f}) - \mathbf{x}^*_{\eta_f} \tag{S.1}$$

such that

$$G_{\eta_f}(0) = 0. \tag{S.2}$$

We denote the fixed point of G_η by

$$\mathbf{y}^*_\eta := \mathbf{x}^*_\eta - \mathbf{x}^*_{\eta_f}. \tag{S.3}$$

Furthermore we define the relaxation map

$$H_\eta(\mathbf{y} - \mathbf{y}^*_\eta) := G_\eta(\mathbf{y}) - \mathbf{y}^*_\eta \tag{S.4}$$

which has the property that $\lim_{t\to\infty} H^t_\eta(\mathbf{y}) = 0$. Let

$$\mathbf{y}(t=0) = \mathbf{y}^*_{\eta_1}, \tag{S.5}$$

for $0 < t \le t_w$

$$\mathbf{y}(t) = G^t_{\eta_2}(\mathbf{y}(t=0)) = G^t_{\eta_2}(\mathbf{y}^*_{\eta_1}) = \mathbf{y}^*_{\eta_2} + H^t_{\eta_2}(\mathbf{y}^*_{\eta_1} - \mathbf{y}^*_{\eta_2}) \tag{S.6}$$

and for $t > t_w$

$$\mathbf{y}(t) = G^{t-t_w}_{\eta_f}(\mathbf{y}(t_w)) = G^{t-t_w}_{\eta_f}(\mathbf{y}^*_{\eta_2} + H^{t_w}_{\eta_2}(\mathbf{y}^*_{\eta_1} - \mathbf{y}^*_{\eta_2})) = H^{t-t_w}_{\eta_f}(\mathbf{y}^*_{\eta_2} + H^{t_w}_{\eta_2}(\mathbf{y}^*_{\eta_1} - \mathbf{y}^*_{\eta_2})) \tag{S.7}$$

where the last line follows from $\mathbf{y}^*_{\eta_f} = 0$. So far we have only formulated the dynamics of the system and Eq. (S.7) is exact. Assuming that the changes of the noise strength $\eta_1 - \eta_f$ and $\eta_2 - \eta_f$ are small, of order ε, and neglecting all terms of higher order than ε we rederive Eq. (2), cf. Sec. II.

In a different approach we keep the full dependence on the changes of the noise strength by now. We replace $H^{t-t_w}_{\eta_f}$ by its linearization $\left[H^{t-t_w}_{\eta_f}\right]^L$ such that Eq. (S.7) becomes

$$\begin{aligned}\mathbf{y}(t) &\approx \left[H^{t-t_w}_{\eta_f}\right]^L(\mathbf{y}^*_{\eta_2}) + \left[H^{t-t_w}_{\eta_f}\right]^L(H^{t_w}_{\eta_2}(\mathbf{y}^*_{\eta_1} - \mathbf{y}^*_{\eta_2})) \approx H^{t-t_w}_{\eta_f}(\mathbf{y}^*_{\eta_2}) + \left[H^{t-t_w}_{\eta_f}\right]^L(H^{t_w}_{\eta_2}(\mathbf{y}^*_{\eta_1} - \mathbf{y}^*_{\eta_2})) \\ &= \mathbf{y}_{2f}(t - t_w) + \left[H^{t-t_w}_{\eta_f}\right]^L(H^{t_w}_{\eta_2}(\mathbf{y}^*_{\eta_1} - \mathbf{y}^*_{\eta_2}))\end{aligned} \tag{S.8}$$

Furthermore we also replace the map $H^{t_w}_{\eta_2}$ by its linearization $\left[H^{t_w}_{\eta_2}\right]^L$ and hence Eq. (S.8) becomes

$$\mathbf{y}(t) = \mathbf{y}_{2f}(t - t_w) + \left[H^{t-t_w}_{\eta_f}\right]^L(\left[H^{t_w}_{\eta_2}\right]^L(\mathbf{y}^*_{\eta_1})) - \left[H^{t-t_w}_{\eta_f}\right]^L(\left[H^{t_w}_{\eta_2}\right]^L(\mathbf{y}^*_{\eta_2})). \tag{S.9}$$

We denote the eigenvalues of $\left[H^t_\eta\right]^L$ by $\lambda^{\eta,t}_1 \ge \lambda^{\eta,t}_2 \ge \cdots \ge \lambda^{\eta,t}_n$ and the corresponding eigenvectors by $\mathbf{v}^{\eta,t}_1, \mathbf{v}^{\eta,t}_2, \ldots, \mathbf{v}^{\eta,t}_n$. For $t = t_w$ we assume a separation of time scales, property (i) which is checked numerically below, that means

$$\lambda^{\eta,t_w}_1 \gg \lambda^{\eta,t_w}_2. \tag{S.10}$$

Therefore we can assume that at t_w only the first eigenvector is relevant and all others are much smaller, thus

$$\left[H_{\eta_2}^{t_w}\right]^L(\mathbf{y}) = \sum_{k=1}^{n} \lambda_k^{\eta_2,t_w}(\mathbf{y}\cdot\mathbf{v}_k^{\eta_2,t_w})\mathbf{v}_k^{\eta_2,t_w} \approx \lambda_1^{\eta_2,t_w}(\mathbf{y}\cdot\mathbf{v}_1^{\eta_2,t_w})\mathbf{v}_1^{\eta_2,t_w} \tag{S.11}$$

We further assume that the eigenvector belonging to the largest eigenvalue is not sensitive to moderate changes in η and t, property (ii) which is checked numerically below. That means we assume that

$$\mathbf{v}_1^{\eta_2,t_w} \approx \mathbf{v}_1^{\eta_f,\tilde{t}} \tag{S.12}$$

when $\tilde{t}$ has the same order of magnitude as t_w. Then we choose $\tilde{t}$ such that

$$\lambda_1^{\eta_2,t_w} = \lambda_1^{\eta_f,\tilde{t}} \tag{S.13}$$

and hence from Eq. (S.11) we obtain

$$\left[H_{\eta_2}^{t_w}\right]^L(\mathbf{y}) \approx \lambda_1^{\eta_2,t_w}(\mathbf{y}\cdot\mathbf{v}_1^{\eta_2,t_w})\mathbf{v}_1^{\eta_2,t_w} \approx \lambda_1^{\eta_f,\tilde{t}}(\mathbf{y}\cdot\mathbf{v}_1^{\eta_f,\tilde{t}})\mathbf{v}_1^{\eta_f,\tilde{t}} \approx \left[H_{\eta_f}^{\tilde{t}}\right]^L(\mathbf{y}). \tag{S.14}$$

Plugging this expression into Eq. (S.9) we obtain

$$\begin{aligned}
\mathbf{y}(t) =& \mathbf{y}_{2f}(t-t_w) + \left[H_{\eta_f}^{t-t_w}\right]^L(\left[H_{\eta_f}^{\tilde{t}}\right]^L(\mathbf{y}_{\eta_1}^*)) - \left[H_{\eta_f}^{t-t_w}\right]^L(\left[H_{\eta_f}^{\tilde{t}}\right]^L(\mathbf{y}_{\eta_2}^*)) \\
\approx& \mathbf{y}_{2f}(t-t_w) + H_{\eta_f}^{t-t_w}(H_{\eta_f}^{\tilde{t}}(\mathbf{y}_{\eta_1}^*)) - H_{\eta_f}^{t-t_w}(\left[H_{\eta_f}^{\tilde{t}}(\mathbf{y}_{\eta_2}^*)\right) \\
=& \mathbf{y}_{2f}(t-t_w) + \mathbf{y}_{1f}(t+\tilde{t}-t_w) - \mathbf{y}_{2f}(t+\tilde{t}-t_w)
\end{aligned} \tag{S.15}$$

Resubstituting $\mathbf{y}$ according to Eq. (S.1) and introducing the abbreviation

$$\hat{t} := t_w - \tilde{t} \tag{S.16}$$

we obtain Eq. (7).

The basic assumptions in the derivation of Eq. (7) are properties i) and ii) that are mathematically given by the conditions (S.10) and (S.12). In the letter, we have argued intuitively that these assumptions should be valid in the present system. For the example presented in Fig. 2 we can also explicitly verify those conditions numerically. The time evolution map F is explicitly given by Eq. (1). Evolving the system for a very long time we obtain the stable fixed point of the map. Thus we can also evolve the map H, cf. Eq. (S.4).

To verify condition (S.10) we need to obtain the eigenvalues $\lambda_i^{\eta,t}$ of $[H_\eta^t]^L$. As a rough estimate we can instead calculate the eigenvalues λ_i^η of $[H_\eta]^L$ and assume $\lambda_i^{\eta,t} \sim (\lambda_i^\eta)^t$. Given the fixed point of the system, the linearization of H_η can be performed analytically. For the parameters of Fig. 2 we obtain for the two largest eigenvalues

$$(\lambda_1^{\eta_2})^{t_w} \approx 8.2\times10^{-2} \gg (\lambda_2^{\eta_2})^{t_w} \approx 1.6\times10^{-7}. \tag{S.17}$$

Thus our assumption (S.10) is valid.

To verify the condition (S.12) we use a robust numerical procedure to obtain the largest eigenvalue and the corresponding eigenvector of $[H_\eta^t]^L$ [S1]. For parameters like in Fig. 2 we find that Eq. (S.13) is valid for $\tilde{t} = 408$. Knowing $\tilde{t}$ we can calculate the scalar product of the normalized eigenvectors $\mathbf{v}_1^{\eta_2,t_w}\cdot\mathbf{v}_1^{\eta_f,\tilde{t}} \approx 0.963$ which indicates that the eigenvector $\mathbf{v}_1$ did not change a lot and Eq. (S.12) is a reasonable assumption.

As we have predicted the value of $\tilde{t}$ we can also calculate the time shift $\hat{t} = 337$ according to Eq. (S.16). In Fig. 2 we used the time shift $\hat{t} = 332$ that was chosen such that the Kovacs-hump has the correct value at $t = t_w$. Hence our numerical prediction for $\hat{t}$ deviates by about 1% from the correct value. This is not surprising since the assumption (S.12) is not satisfied perfectly and also the linearization of H_η^t might introduce some deviations.

Our result (7) describes a relation between vectors of all Fourier modes. Thus it is holding not only for the polar order parameter $\Psi = \pi g_1$ which corresponds to the first Fourier mode but it is much more general. In Fig. S1 we show the relaxation curves and the Kovacs-hump of the second Fourier mode following the same Kovacs-protocol as the order parameter in Fig. 2. We find that the relation (7) fits the data well using the same time shift $\hat{t}$ as in Fig. 2.

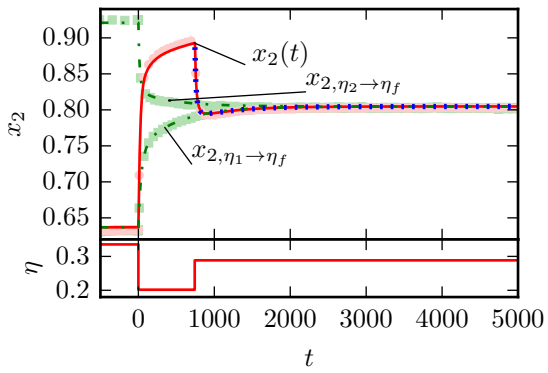

FIG. S1. The relaxation curves $x_{2,\eta_1\to\eta_f}(t)$, $x_{2,\eta_2\to\eta_f}(t)$ (dash-dotted line) and the Kovacs-hump $x_2(t)$ (solid red line) of the second Fourier mode g_2 obtained from the kinetic theory (1) are in good agreement with agent-based simulations (light green squares and light red circles, respectively). The nonlinear theory (7) with the same time shift as in Fig. 2, $\hat{t} = 332$, (dotted blue line) fits well. Parameters are as in Fig. 2.

LINEAR THEORY

We assume that

$$\eta_1 - \eta_f = a_1\varepsilon, \qquad \eta_2 - \eta_f = a_2\varepsilon, \tag{S.18}$$

where ε is small and a_1 and a_2 are of similar size, $a_1, a_2 \sim 1$. We expand the fixed points

$$\mathbf{y}^*_{\eta_1} = \varepsilon a_1 \mathbf{y}^*_0 + \mathcal{O}(\varepsilon^2), \qquad \mathbf{y}^*_{\eta_2} = \varepsilon a_2 \mathbf{y}^*_0 + \mathcal{O}(\varepsilon^2) \tag{S.19}$$

for some constant vector $\mathbf{y}^*_0$. Inserting these fixed points into the exact expression (S.7) we obtain

$$\begin{aligned}\mathbf{y}(t) &= H_{\eta_f}^{t-t_w}(\varepsilon a_2 \mathbf{y}^*_0 + H_{\eta_2}^{t_w}(\varepsilon(a_1-a_2)\mathbf{y}^*_0 + \mathcal{O}(\varepsilon^2)) + \mathcal{O}(\varepsilon^2)) \\ &= H_{\eta_f}^{t-t_w}(\varepsilon[a_2\mathbf{y}^*_0 + (a_1-a_2)([H_{\eta_2}]^L)^{t_w}(\mathbf{y}^*_0)] + \mathcal{O}(\varepsilon^2)),\end{aligned} \tag{S.20}$$

where $[H_{\eta_2}]^L$ denotes the linearization of H_{η_2}. The linear map $[H_{\eta_2}]^L$ depends on ε via η_2 and thus we can expand it for small ε. Only the leading term is necessary since we neglect terms of order ε^2. Thus we obtain

$$\mathbf{y}(t) = H_{\eta_f}^{t-t_w}(\varepsilon[a_2\mathbf{y}^*_0 + (a_1-a_2)([H_{\eta_f}]^L)^{t_w}(\mathbf{y}^*_0)] + \mathcal{O}(\varepsilon^2)). \tag{S.21}$$

Since the map $[H_{\eta_2}]^L$ is applied t_w times, terms of order ε^2 come with a prefactor of t_w. Therefore they can be neglected only if $1/\varepsilon \gg t_w$. For not too small changes in η and long waiting times this assumption is not maintainable and the linear theory cannot be applied. This is the reason why Eq. (2) fails completely for long waiting times.

Continuing the expansion of Eq. (S.21) for small ε we obtain

$$\begin{aligned}\mathbf{y}(t) &= \varepsilon([H_{\eta_f}]^L)^{t-t_w}(a_2\mathbf{y}^*_0 + (a_1-a_2)([H_{\eta_f}]^L)^{t_w}(\mathbf{y}^*_0)) + \mathcal{O}(\varepsilon^2) \\ &= \frac{a_2}{a_1}([H_{\eta_f}]^L)^{t-t_w}(\varepsilon a_1 \mathbf{y}^*_0) + \frac{a_1-a_2}{a_1}([H_{\eta_f}]^L)^{t_w}(\varepsilon a_1 \mathbf{y}^*_0) + \mathcal{O}(\varepsilon^2) \\ &= \frac{a_2}{a_1}\mathbf{y}_{1f}(t-t_w) + \frac{a_1-a_2}{a_1}\mathbf{y}_{1f}(t) + \mathcal{O}(\varepsilon^2)\end{aligned} \tag{S.22}$$

Evaluating this equation at $t = 0$, resubstituting $\mathbf{x}$ according to Eq. (S.3) and observing only $x_1 = \Psi/\pi$ we find γ according to Eq. (3) as

$$\gamma = \frac{a_2}{a_2 - a_1}. \tag{S.23}$$

With this abbreviation Eq. (S.22) becomes

$$\mathbf{y}(t) = \frac{1}{1-\gamma}\mathbf{y}_{1f}(t) - \frac{\gamma}{1-\gamma}\mathbf{y}_{1f}(t-t_w). \tag{S.24}$$

From the first vector component of this equation we obtain Eq. (2). Thus we rederived the linearized theory [43] in the context of time-discrete dynamical systems.

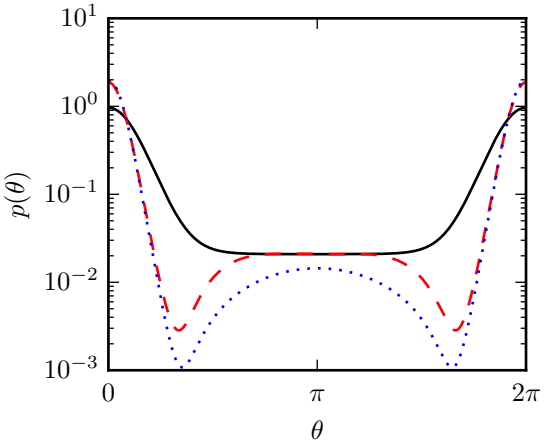

FIG. S2. Angular probability density $p(\theta)$ during the Kovacs-protocol at different times before $t_w = 745$: $t = 0$ (black solid line), $t = 100$ (red dashed line) and $t = 700$ (blue dotted line). Parameters like in Fig. 2.

SLOW RELAXATION MECHANISM

In this section, we discuss the slow relaxation mechanism that leads to strong memory effects. In Fig. S2, we display snap shots of the angular probability density at times $t = 0, 100, 700 < t_w$ following the relaxation from η_2 to η_f which is the first part of the Kovacs-protocol presented in Fig. 2. The direction of the majority of the particles is centered around $(0 \mod 2\pi)$. After $t = 100$ this dominating peak is already relaxed towards its steady state shape. However, there is a small population of particles that move in the opposite direction $\theta = \pi$. Due to the bounded confidence interaction rule, these particles do not interact with the large group of particles that move in direction $\theta = 0$. Therefore they reorient mainly due to noise. If the noise strength is small, this process is very slow and it takes a long time until the population moving into direction $\theta = \pi$ has reorientated and the system has reached its steady state. Apparently this noise driven mechanism is the slowest relaxation mode of the system. Moderate changes of the noise strength change the relaxation speed significantly, however, the noise driven reorientation of a minor population remains the slowest relaxation mode of the system.

COEFFICIENTS AND NUMERICAL PARAMETERS

We give the coefficients of Eq. (1), cf. Refs. [27, 29] for a derivation. They depend on the noise strength η, the average number of other particles within interaction distance M and the maximal angular difference α between two particles directions that still leads to interactions.

$$\lambda_k(\eta, M) = \frac{\sin(k\eta/2)}{1+M}\frac{4}{k\eta}, \qquad A_k(M,\alpha) = \frac{1}{2} + x_0 M\big\{\pi - \alpha + \frac{3}{k}\sin(k\alpha/2) - \frac{1}{2k}\sin(k\alpha)\big\},$$
$$B_{kq}(M,\alpha) = \frac{M}{2}\alpha\big\{\,\mathrm{sinc}[(k/2-q)\alpha/\pi] - \mathrm{sinc}(q\alpha/\pi)\big\}, \qquad C_{kq}(M,\alpha) = \frac{M}{2}\alpha\big\{\,\mathrm{sinc}[(k/2+q)\alpha/\pi] - \mathrm{sinc}(q\alpha/\pi)\big\}.$$

In Figs. 1 and 2 we compare the kinetic theory (1) with agent-based simulations. We simulated at $M = 0.2$, where the low density approximation is not perfect. Therefore, the order parameter is slightly different in agent-based simulations. For a better comparison with the kinetic theory we used minimally different noise strengths in the simulations, such that the steady state order parameter coincides with the kinetic theory. We used for Fig. 1 $\eta_1 = 0.38$, $\eta_2 = 0.46$, $\eta_f = 0.395$ and for Fig. 2 $\eta_1 = 0.34$, $\eta_2 = 0.197$ and $\eta_f = 0.29$.

We obtained the data of Fig. 3 by numerically integrating Eqs. (6a) and (6b) of Ref. [37]. We used the parameters $\alpha = 0.3$ and $d = 2$. We followed the Kovacs-protocol with waiting time $t_w = 1.864$ and stationary temperatures $T_{s,2} = 10^{-4/3} \cdot T_{s,1}$ and $T_{s,f} = (1.01)^{4/3} \cdot T_{s,2}$. The absolute value of $T_{s,1}$ is not relevant, since we investigate only relative quantities, cf. Ref. [37] for more details. In Fig. 3 we present $\beta = \sqrt{\frac{T_{s,2}}{T}}$.

DRIVEN GRANULAR GAS

In this section we discuss the application of Eq. (7) to the driven granular gas of Ref. [37]. In order to apply Eq. (7), properties (i) and (ii) must be satisfied. In order to fulfill these conditions we have chosen the steady state granular temperatures $T_{s,2}$ and $T_{s,f}$ close to each other. This way, we achieve a long waiting time since the steady state order parameter at $T_{s,2}$ is very close to the one of $T_{s,f}$ and therefore the system is almost completely relaxed at t_w. Hence, it is a reasonable assumption that all but the slowest eigenmodes have already completely relaxed and property (i) is justified. Property (ii) is clearly justified with good approximation when $T_{s,2}$ and $T_{s,f}$ are chosen close enough to each other, because then the dynamics is changed only a little and the slowest eigenmodes remain almost constant. Here, we can also assume that the corresponding eigenvalues are almost the same and therefore $\hat{t} \approx 0$. Thus, when $T_{s,2}$ and $T_{s,f}$ are chosen close enough together, properties (i) and (ii) are valid and therefore Eq. (7) is applicable. By this choice of stationary granular temperatures we expect only a small Kovacs-effect. However the Kovacs-effect reported in Ref. [37] is very small for all choices of parameters anyway.

The interesting feature of this particular system is that the Kovacs-hump can have the opposite sign. This property can be understood investigating Eq. (7). Since $T_{s,2}$ is close to $T_{s,f}$ and $\hat{t} \approx 0$ it is clear that the term $\mathbf{x}_{2f}(t)$ is almost constant for large t. Taking the time derivative of Eq. (7) on the right-hand side only the terms $\mathbf{x}'_{2f}(t - t_w)$ and $\mathbf{x}'_{1f}(t)$ remain. They carry the opposite sign. Which of them is dominating determines the sign of the Kovacs-effect. Apparently both cases are possible depending on parameters.

[S1] To determine the largest eigenvalue of $[H^t_\eta]^L$ we fix a small parameter δ, here $\delta = 0.01$. We start with the initial vector $\mathbf{x}$ given by $x_1 = 1$ and $x_i = 0$ for $i > 1$. We then replace $\mathbf{x}$ by $H^t_\eta(\delta \cdot \mathbf{x})/||H^t_\eta(\delta \cdot \mathbf{x})||$, such that always $||\mathbf{x}|| = 1$. This step is repeated many times. In this way all eigenvectors but the one that corresponds to the largest eigenvalue decay. Eventually $\mathbf{x}$ converges and the largest eigenvalue is obtained by $\lambda_1^{\eta,t} = ||H^t_\eta(\delta \cdot \mathbf{x})||/\delta$ and $\mathbf{x}$ is the corresponding eigenvector.